Retraction

Retracted: Research on Vessel Speed Heading and Collision Detection Method Based on AIS Data

Mobile Information Systems

This article has been retracted by Hindawi following an investigation undertaken by the publisher [1]. This investigation has uncovered evidence of one or more of the following indicators of systematic manipulation of the publication process:

(1) Discrepancies in scope

(2) Discrepancies in the description of the research reported

(3) Discrepancies between the availability of data and the research described

(4) Inappropriate citations

(5) Incoherent, meaningless and/or irrelevant content included in the article

(6) Peer-review manipulation

The presence of these indicators undermines our confidence in the integrity of the article's content and we cannot, therefore, vouch for its reliability. Please note that this notice is intended solely to alert readers that the content of this article is unreliable. We have not investigated whether authors were aware of or involved in the systematic manipulation of the publication process.

Wiley and Hindawi regrets that the usual quality checks did not identify these issues before publication and have since put additional measures in place to safeguard research integrity.

We wish to credit our own Research Integrity and Research Publishing teams and anonymous and named external researchers and research integrity experts for contributing to this investigation.

The corresponding author, as the representative of all authors, has been given the opportunity to register their agreement or disagreement to this retraction. We have kept a record of any response received.

References

[1] G. Wang, E. Fan, G. Zheng, K. Li, and H. Huang, "Research on Vessel Speed Heading and Collision Detection Method Based on AIS Data," *Mobile Information Systems*, vol. 2022, Article ID 7257075, 10 pages, 2022.

Research Article

Research on Vessel Speed Heading and Collision Detection Method Based on AIS Data

Guoqing Wang [ID],[1,2] En Fan,[3] Guohua Zheng,[1] Kexiang Li,[1] and Haiguang Huang[4]

[1]*Zhejiang Suosi Technology Co. Ltd, Wenzhou 325000, Zhejiang, China*
[2]*Asia Pacific University of Technology and Innovation, Technoloy Park Malaysia, 57000 Kuala Lumpur, Malaysia*
[3]*Department of Computer Science and Engineering, Shaoxing University, Shaoxing 312000, Zhejiang, China*
[4]*College of Computer Science and Artificial Intelligence, Wenzhou University, Wenzhou 325000, Zhejiang, China*

Correspondence should be addressed to Guoqing Wang; wgq@zjsos.net

In order to better predict the sailing information data of fishing boats, make accurate prediction and spacing budget for the sailing status of ships, achieve more accurate coordination and early warning in advance, and ensure the safety of fishing boats' laneway, the essay combined the kinematics equation and artificial neural network model to adapt to the traffic situation of fishing boats in the far sea. A course and collision test technique based on ship AIS data is proposed, and the course collision detection method of fishing boats is studied by means of actual ship beacon collision accident data. Through the practical test, taking the navigation mark 4560.117 as an example, under the detection track of the navigation mark field corresponding to $R = 70$, the two ships have the same track, thus verifying the practicality and feasibility of the ship navigation mark collision detection method.

1. Introduction

In recent years, with the rapid development of China's economy, shipping industry has also developed rapidly. Due to the increasing volume of shipping traffic, the situation of waterway congestion and navigation accidents gradually increased in the shipping area, and even caused huge economic losses. In this case, it is better to predict the propagation trajectory accurately. On the one hand, it can timely find the abnormal trajectory of the ship. On the other hand, it can also effectively prevent ship landing, avoid collision accidents, and provide reliable technical support for the scientific decision-making of fishing vessel collision avoidance and route planning. In order to better strengthen the scientific control and monitoring of maritime shipping traffic, AIS technology began to emerge. This technology, through automatic identification system, can break the disadvantages of traditional radar equipment, has higher positioning accuracy for ships, and is less affected by terrain, weather, and other factors. It can provide reliable data support for ship navigation gathering prediction and collision avoidance.

2. Literature Review

Some scholars proposed a four-element dynamic ship domain model, improved the method of judging safe distance and collision risk with the help of AIS information, and established a set of reasonable and effective ship collision avoidance decision model. It realizes the judgment of collision danger and encounter situation. Some scholars have also made corresponding discussions on collision avoidance of ships and postulated that the AIS system is an effective means to avoid collision. The AIS system in ships will accurately detect the changes in course and speed caused by weather or human factors, which helps ships to determine whether they will encounter the scene; based on dynamic AIS information, an adaptive ship safety domain system with spatial risk function is proposed to identify collision and landing risks, which greatly improves the accuracy of identifying collisions between ships [1]. Some scholars extracted the motion model from the original AIS data and used it to construct the corresponding motion anomaly detector. Gaussian filter and tracking filter are

Table 1: Composition of AIS data structure of ships.

Static data	Dynamic data	Voyage data
MMSI unique identifier	Ground course	The depth of the draft
Callsign hull number	Speed of sailing	The port of destination
Ship type	Longitude	Eta.
The length and breadth of the ship	Latitude	None

Table 2: AIS data information table of ships.

The field names	Field description	The field type	Note
ID	Record line account	Integer	The static message
Ship_ jid	The ship number	Integer	The static message
IMO	IMO ship number	String	The static message
Name	Name of vessel	String	The static message
Callsign	Call sign of ship	String	The static message
Ship_ type	Ship type	Integer	The static message

used to predict ship motion. An incremental learning of ship motion patterns for single AIS ground receivers, regional networks, or global scale tracking is proposed. By providing the relevant characteristics of ship traffic to detect ship anomaly trajectory, ideas for many ship anomaly detection models proposed by many subsequent scholars are provided. Abnormal ship track can be detected from AIS and recorded by feature learning algorithm. This detection method can effectively detect abnormal trajectory and provide an important basis for the realization of maritime intelligent transportation [2]. Some scholars proposed a clustering algorithm related to regional density. However, the neighborhood radius of this method limits the number of line segments required in the clustering process. In order to solve this problem, the algorithm is improved to produce an algorithm that can output many same clustering trajectory segments. However, for a wider range of decision parameters, this method may encounter problems in data sets with circular motion and frequent crossing paths. The DBSCAN algorithm is proposed to cluster ship track, which provides ideas for many subsequent scholars in the study of ship track clustering. The DBSCAN algorithm is improved and a trajectory clustering model based on AIS data is proposed to analyze ship track. The improved density-based DBSCAN clustering algorithm can automatically classify different routes with route characteristics and improve the clustering accuracy of main route extraction of ship track. A probabilistic method based on hidden Markov model is proposed for ship trajectory clustering. This model provides a natural framework, and models the inherent time correlation of data according to the definition, and displays it visually [3, 4].

3. AIS Data Preprocessing and Choice of Flight Path Prediction Model

3.1. Data Structure. AIS has become an essential component of modern ship navigation system. AIS information mainly contains three types of data, namely, static data of ships,

dynamic data of ships, and navigation data of ships. Specific data information is shown in Table 1.

These information parameters representing ship navigation state are of great value to the study of ship track prediction. Therefore, detailed analysis of AIS internal data is needed. AIS data update speed is very fast, which can provide real-time dynamics of ships [5, 6]. In order to facilitate the analysis of AIS data information structure and types, the basic format of AIS data is given, as shown in Table 2.

3.2. AIS Data Preprocessing

3.2.1. AIS Data Collection. Ship track prediction is to predict the course of the ship in the next period according to the track of the ship, so it is necessary to obtain the known historical track data. However, currently available AIS data record the track data of all ships, and does not classify and encode individual ship routes, so the track data of a single ship route cannot be directly obtained, and the ship route needs to be identified artificially according to the MMSI unique identification code of ship AIS data. Filter and sort according to MMSI and collection time. Sample table of collected and sorted AIS data is shown in Table 3.

3.2.2. AIS Data Cleaning. The AIS system identifies a ship by the unique identification code MMSI. Based on time series, it is necessary to perform certain data cleaning and processing in case of the following special situations for the ship track data encoded only by MMSI [7].

(1) Illegal data. Illegal data refer to data with multiple round trips at multiple places in the sea area or with large time difference between the ship and the ship due to man-made or environmental reasons. In this case, a clean and stable track period can be selected according to the ship's time interval, speed, and heading as the input data of the track pre-model.

TABLE 3: Partial AIS data collected.

Ship identification code	Time	Latitude	Longitude	Speed of sailing	Heading course
367617230	2017-12-00:00:22	19.30434	−65.4934	11.4	96
367617230	2017-12-0100:01:33	28.30358	−65.4395	11.23	56
367617230	2017-12-0100:06:03	16.30284	−65.4257	11.00	91
367617230	2017-12-0100:07:12	15.30138	−65.4188	11.96	90

(2) Drift data. Drift data refer to some abnormal data points that deviate far from the normal course due to positioning errors. In case of drift trajectory data, this point is usually filled by fitting according to the distance between the two points before and after. For data points that cannot be fitted, they can be directly removed.

(3) Sparse data. Sparse data refer to the data with a large distance between two adjacent track points due to information loss. These kind of data need to be discarded directly. In fact, in the COLLECTED AIS data, some track points are close to each other or close to the same straight line. Such data should be processed by compression with appropriate time interval [8].

3.2.3. AIS Data Missing Value Processing. Assume that the ship's track sequence is shown in equation (1):

$$
\begin{aligned}
T &= \left\{ p_t^1, p_t^2, \cdots, p_t^n \right\}, \\
p_t^i &= \{ \text{sog}, \text{cog}, \text{lat}, \text{lon} \},
\end{aligned} \tag{1}
$$

p_t^i represents THE AIS data at time t_i, where sog, cog, lat, lon, respectively, represent the ship's speed, heading, latitude, and longitude at time t. Interpolation methods for ship track data can be roughly divided into the following categories:

First, linear interpolation.

Set the position coordinates of the missing data point as (t_i, p_t^i), and the position coordinates of the front and rear data points as (t_{i-1}, p_t^{i-1}) and (t_{i+1}, p_t^{i+1}), respectively. The missing values are fitted by the coordinate data of the front and rear data points, and the specific linear interpolation fitting diagram is shown in Figure 1.

According to Figure 1, the interpolation formula can be expressed as follows:

$$
p_t^i = p_t^{i-1} + \frac{p_t^{i+1} - p_t^{i-1}}{t_{i+1} - t_{i-1}} (t_i - t_{i-1}). \tag{2}
$$

It can be seen from the above equation that the linear interpolation method is only applicable to the trajectory data with a small degree of bending. If the trajectory curvature is large, this method will produce relatively large errors.

Second, Lagrange interpolation.

Assume that the coordinates of $k+1$ observed track points of the ship can be expressed as formula (3):

$$
\left(t_0, p_t^0 \right), \left(t_1, p_t^1 \right), \cdots, \left(t_k, p_t^k \right). \tag{3}
$$

Suppose that the position of the ship is different at any two moments, t_i represents the corresponding time point of
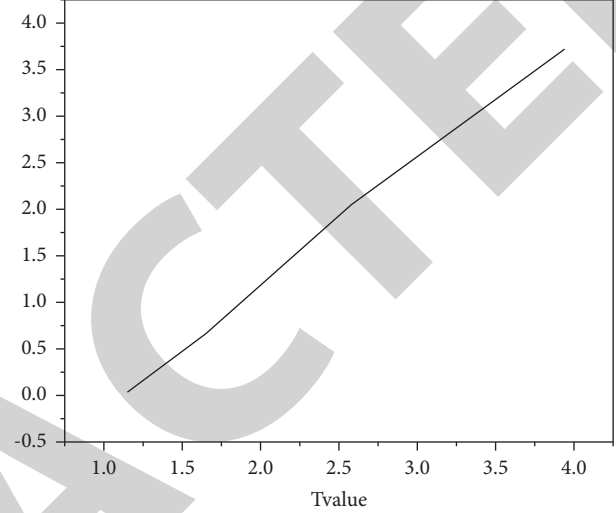

FIGURE 1: Schematic diagram of linear interpolation.

the data, and p_t^i represents the value of the ship at the corresponding time point. The Lagrange interpolation polynomial can be expressed as formula (4):

$$
L(t) = \sum_{i=0}^{k} p_t^i l_i(t_i), \tag{4}
$$

where $l_i(t)$ represents the interpolation basis function, and its expression is equation (5):

$$
l_i(t) = \prod_{j=0, i \neq j}^{k} \frac{t - t_j}{t_i - t_j}. \tag{5}
$$

The value of the above formula is 1 at $t = t_i$ and 0 at $t \neq t_i$, so the polynomial can be guaranteed to pass through all observed data points. Because polynomials can fit curves well, this method is more suitable for trajectory interpolation of curved ships.

3.3. Track Prediction Model Based on PSO-LSTM. PSO algorithm is a heuristic global search algorithm based on swarm intelligence. The algorithm compares the optimization problem to bird predation, and the optimal solution is the target food. Each bird is the particle in THE PSO algorithm, and all the particles move at a certain speed and track in space, and guide the behavior of the whole population to approach the target function through the function to be optimized [9]. Its essence is to use individual competition mechanism to generate local optimal solution, and then through information sharing and cooperation

mechanism to generate global optimal solution. The specific process is shown in Figure 2.

PSO algorithm is a method to search for the optimal solution globally. The combination of PSO algorithm and LSTM network can help the model to determine the optimal parameter combination and achieve better prediction effect. Set the number of parameter combinations in LSTM neural network as N, that is, a population composed of N particles is formed. The position of each particle i at any time is an n-dimensional space vector, so the position of particle i at the t-th time period can be represented by equation (6):

$$x_i(t) = [x_{i1}(t), x_{i2}(t), \cdots, x_{in}(t)]^T. \tag{6}$$

Fitness function determines the direction of particle swarm, which is set as mean square error, as shown in equation (7):

$$F = \sum_{i=1}^{n} |y_i - y_i'|, \tag{7}$$

where y_i is the expected value of the i th particle, and y' is the corresponding predicted value.

In the update stage, the historical optimal x_i^{pb} set at t time cycles is expressed in formulas (8)–(10):

$$x_i^{pb}(t) = [x_{i1}^{pb}(t), x_{i2}^{pb}(t), \cdots, x_{in}^{pb}(t)]^T. \tag{8}$$

The historical optimum of all particles is x_i^{gb}:

$$x_i^{gb}(t) = [x_{i1}^{gb}(t), x_{i2}^{gb}(t), ..., x_{in}^{gb}(t)]^T. \tag{9}$$

Then, in the t time period, the updating formula of the individual extreme value x_i^{pb} of particle i is:

$$x_i^{pb}(t+1) = \begin{cases} x_i(t+1), & F(x_i(t+1)) \le Fx_i^{pb}(t), \\ x_i^{pb}(t), & F(x_i(t+1)) \le Fx_i^{pb}(t). \end{cases} \tag{10}$$

The updating formula of the global extreme value x_i^{gb} of all particles is equation (11):

$$x_i^{gb}(t+1) = \arg\{F_{\min}(x_i^{gb}(t+1))\}, \tag{11}$$

where arg is the value of independent variable x corresponding to function $F(x)$. The velocity and position of the particle in the $(t+1)$ time period are updated by formulas (12) and (13):

$$v_i(t+1) = l \cdot v_i(t) + c_1 \cdot r_1 \cdot (x_i^{pb}(t) - x_i(t)) + c_2 \cdot r_2 \cdot (x_i^{gb}(t) - x_i(t)), \tag{12}$$

$$x_i(t+1) = x_i(t) + v_i(t+1), \tag{13}$$

where, $v_i(t)$ is the traveling speed of particle i in the t time period; l is the linear decreasing weight coefficient; c_1、c_2 represent learning factor; r_1、r_2 is a uniform random number whose value range is $(0, 1)$. After the particle has obtained the best fitness, the corresponding parameter combination can be put into the LSTM neural network.
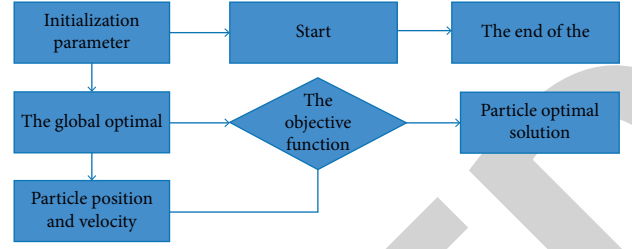

Figure 2: Basic flow of PSO algorithm.

3.4. GA-LSTM Prediction Model. GA algorithm is a computational model of evolutionary process inspired by biological evolution theory and natural genetics principle. It is a global, parallel, and efficient search method in essence. When dealing with related problems, GA algorithm will transform them into the biological evolution process, which will be eliminated according to the survival of the fittest principle. Finally, the evolution model will converge to the optimal individual, namely, the optimal solution of the problem [10]. The specific process is shown in Figure 3.

In the fitness calculation stage, GA algorithm is consistent with PSO algorithm, and the mean square error is used to evaluate the fitness equation (14):

$$F = \sum_{i=1}^{n} |y_i - y_i'|. \tag{14}$$

In the selection stage, Roulette's rule is adopted as the selection operator. This method can improve the evolutionary weight of individuals with high fitness and keep the evolutionary weight of individuals with low fitness not zero, so as to ensure the diversity of parameters in THE LSTM network and avoid the occurrence of local extreme values. Then the probability p_i of individual i being selected in the selection stage is equation (15):

$$p_i = \frac{(k/F_i)}{\sum_{i=1}^{n} (k/F_i)}, \tag{15}$$

where F_i is the fitness value of individual i in the population. In crossover stage, random linear combination of individuals is carried out. The specific real number crossover process is shown in formulas (16) and (17):

$$w_{ij} = w_{ij} \cdot (1 - u) + w_{ij} \cdot u, \tag{16}$$

$$w_{kj} = w_{kj} \cdot (1 - u) + w_{kj} \cdot u, \tag{17}$$

where w_{ij} is the information of j position on the i th gene; w_{kj} is the information of j position on the k th gene; u is the probability of information crossing, and its value ranges from 0 to 1. In the mutation stage, nonuniform mutation is adopted to conduct random perturbation of existing chromosomes, as shown in formulas (18)–(20):

$$w_{ij}' = w_{ij} + (w_{\min} - w_{ij}) \cdot F_{(G_1)}, r_3 \ge 0.5, \tag{18}$$

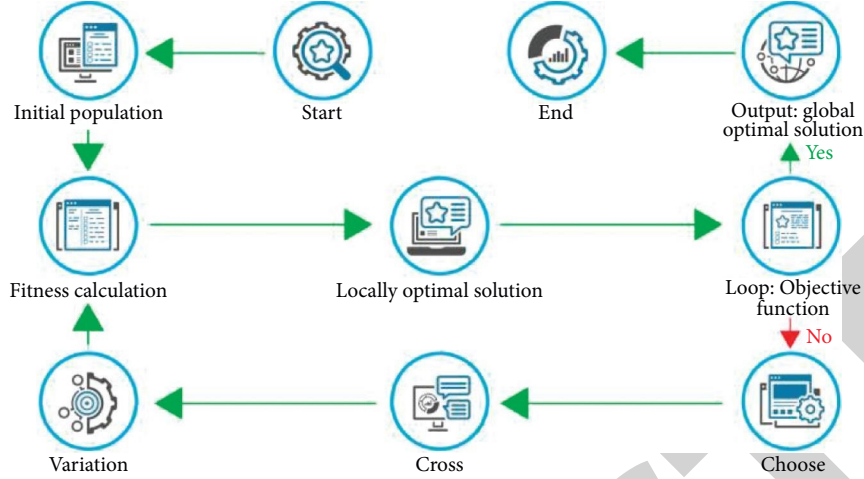$$w_{ij}' = w_{ij} + (w_{ij} - w_{\max}) \cdot F_{(G_1)}, r_3 \ge 0.5, \tag{19}$$

Figure 3: Basic flow of GA algorithm.

$$F_{(G_1)} = r_4 \left(1 - \frac{G_1}{G_2}\right)^2, \tag{20}$$

where w_{ij}' is the new chromosome after mutation; G_1、G_2 are the current generation and the maximum generation; r_3、r_4 are the disturbance probability, and its value range is [0,1]. After the optimal fitness of the population is obtained, the corresponding parameter combination can be put into the LSTM neural network.

3.5. PSO-LSTM Model and GA-LSTM Model. PSO and GA heuristic algorithms are used to adjust the combination of Units, steps, and EPOchs of LSTM network in each time sequence and feature. The experiment sets the voyage prediction timestamp as {1, 5, 10, 20, 30, 40, 50} uniformly to test the prediction effect of the two models in the long and short periods.

Tables 4–6 show the average absolute percentage errors predicted by LSTM model, PSO-LSTM model, and GA-LSTM model for four kinds of navigational dynamics features: longitude, latitude, speed, and heading. Through the horizontal comparison of data, it can be seen that with the addition of the two optimization algorithms, the prediction errors of the LSTM model in the four types of features are reduced to different degrees. Compared with the LSTM model, PSO-LSTM model and GA-LSTM model have better effects on the prediction of longitude, latitude, and speed in the whole time series. The maximum longitude MAPE decreases to 0.0054, and the maximum latitude MAPE decreases to 0.002. Speed MAPE value decreased to 2.9923; for the prediction of heading characteristics, the two optimization algorithms perform well in the short time sequence, and local error oscillation occurs in the long time sequence prediction, and the maximum MAPE value decreases to 0.4428.

Figures 4 and 5 show the root mean square error of PSO-LSTM model and GA-LSTM model for the prediction of speed and heading characteristics in navigation dynamics. It can be seen that the error of the GA-LSTM model is significantly smaller than that of the PSO-LSTM model in the

Table 4: Average absolute percentage error of LSTM prediction model.

MAPE	LON	LAT	SoG	CoG
$n = 1$	0.0012	0.269	1.7896	0.5693
$n = 6$	0.0011	0.369	2.6391	0.1269
$n = 12$	0.0016	0.598	8.2369	0.7863
$n = 20$	0.0018	0.756	9.5630	0.4599

Table 5: Average absolute percentage error of PSO-LSTM prediction model.

MAPE	LON	LAT	SoG	CoG
$n = 2$	0.0002	0.369	3.7897	0.5623
$n = 9$	0.0001	0.349	4.6392	0.1369
$n = 10$	0.0006	0.578	7.2359	0.7767
$n = 30$	0.0008	0.856	8.5637	0.4798

Table 6: Average absolute percentage error of GA-LSTM prediction model.

MAPE	LON	LAT	SoG	CoG
$n = 8$	0.0032	0.268	9.7896	0.5593
$n = 7$	0.0011	0.369	8.6391	0.1369
$n = 13$	0.0056	0.548	4.2369	0.7753
$n = 40$	0.0098	0.736	1.5630	0.4572

prediction of ship speed and heading. Therefore, it can be analyzed that there are multiple optimal solutions for "multi-peak regression" problems such as speed and heading characteristics, and more attention is paid to the global search ability. Compared with PSO algorithm, the GA algorithm has higher complexity, better global optimization, and implicit parallelism, which is reflected in the LSTM model framework as stronger search ability. The unique biological evolution process of the algorithm ensures the diversity of the population and can escape the local peak with a certain probability in the iterative process, avoiding the model falling into the local optimum in the iteration [11, 12].
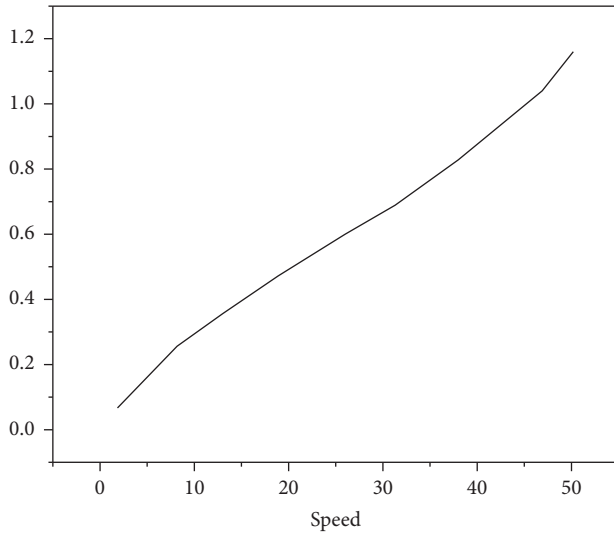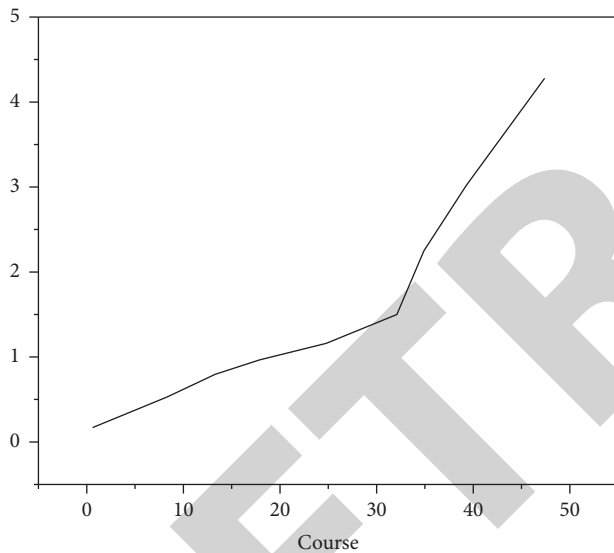
Figure 4: PSO-LSTM model.

Figure 5: Root mean square error of the GA-LSTM model.

To sum up, both PSO algorithm and GA algorithm can enable LSTM-based navigation dynamic prediction model to find more optimal parameters and improve the prediction accuracy. Among them, the PSO-LSTM model performs better in the prediction of longitude and latitude characteristics, and the GA-LSTM model performs better in the prediction of speed and heading characteristics. Therefore, the two algorithms are combined to provide reference for subsequent model comparison, and the new model after combination is denoted as LSTM*.

4. Ship-Beacon Collision Detection Method Based on Hierarchical Navigation Beacon Field

4.1. Principle of Ship-Beacon Collision Detection. According to the construction methods of the ship domain model, it can be divided into ship domain model based on

analysis, ship domain model based on statistical methods, and ship domain model based on intelligent technology. Ship domain based on analysis is mainly expressed as a function expression of ship length, width, and speed. However, due to the influence of ship navigation environment and other aspects of ship domain, ship domain has differences in different waters, resulting in limited portability of the ship domain model. The ship domain model based on intelligent technology integrates fuzzy set theory and neural network technology, and outputs the fuzzy boundary of ship domain by taking the distance between two ships and the relative position as the input of the model. However, because the neural network adopts the "black box" mode to carry out association mapping, the exact relation expression cannot be obtained. The ship domain model construction method based on statistical method is based on maritime observation data, and the ship domain model is constructed by fitting the distribution of ships around the central ship and combining with navigation rules [13]. For example, based on AIS data and network division of the region, single ship grid frequency diagram is extracted by superimposing the distribution of other ships around the central ship, and ship domain model in restricted waters is calculated and analyzed. Therefore, the corresponding ship domain model can be constructed based on AIS data in the situation of designated waters and designated ships [14–16].

Navigation mark is a kind of ship with special purpose in essence. In order to avoid collision with navigational markers, ships in the past keep a safe distance from them in most cases, which means that navigational markers also exist in the realm of ships. Referring to the expression of the ship field, this essay describes it as the navigation mark field. It can be speculated that under normal conditions, the past ships are active in the navigation mark area, and when the ships invade the navigation mark area, they can be considered as suspected of colliding with the navigation mark. On the other hand, in the traditional ship-buoy collision detection method, it is impossible to avoid the situation of missing detection caused by the discontinuous data returned, so the ship-buoy collision detection method based on the navigation buoy field is adopted. Ship suspicion can be judged by detecting whether the ship's navigation track and navigation mark field have intersection, so as to avoid missed detection [17].

At present, the research mainly focuses on the research in the field of ships and less involves the research in the field of navigation markers. Therefore, in order to improve the effectiveness of the ship-beacon collision detection method based on the navigational domain, it is necessary to study the navigational domain first. That is, AIS data under non-accident conditions are taken as the basis. The distribution results of ships in all directions around the navigation mark field were obtained by grid division of the waters near the navigation mark and superposition of the grid distribution of passing ships in the waters near the navigation mark, and the boundary of the navigation mark field was obtained by merging. Then, combined with the model of navigation mark field, the passing ships on the day of navigation mark collision are detected. By judging whether past ships

intruded into the navigation mark area and the extent of intrusion, the suspicious nature of past ships' accidents was determined, and the ships involved were traced, as shown in Figure 6.

4.2. Analysis of the Construction Process in the field of Navigation AIDS. In the field of navigational markers, AIS data of ships are screened through time range and space, and the waters near navigational markers are networked. The distribution of ships in the grid is counted, and the accurate boundary range of navigational markers is obtained by superimposing data of several similar navigational markers, so as to build the navigational domain model.

At the same time, in order to confirm the accurate position of the ship in the waters near the navigation mark, so as to accurately extract the boundary of the navigation mark field, network division is carried out for the waters near navigation markers, and the region is divided into grids with a side length of 10 m [18]. After regional grid division, ships will be in different grids, ships are distributed in different grids, and the corresponding grid frequency increases by 1.

To solve this problem, firstly confirm the scope of the rectangular area where the ship is located and the corresponding grid according to the coordinates of the four vertices of the ship, as shown in the blue rectangular box in Figure7. Then, in order to determine whether each grid in the rectangular frame intersects with the rectangular frame, the separation axis theory is adopted. The separation axis is defined as follows: When polyhedron A and B are projected vertically onto a line L without overlap, the line L is said to be the separation axis of the polyhedron A and B. According to this, there is a separation axis theorem: if and only if polyhedron A and polyhedron B have a separation axis, the closed region formed will not intersect. If there is a separation axis, one of the separation axes must meet one of the following three conditions:

The first condition is that the separation axis is perpendicular to some plane of polyhedron A;

The second condition is that the separation axis is perpendicular to some plane of polyhedron B;

The third condition is that the separation axis is perpendicular to a plane that is parallel to an edge of the convex polyhedron A and an edge of the convex polyhedron B.

Based on the separation axis theorem, the intersection of objects can be determined only by judging whether there is separation axis between objects. When one or more separate axes exist, the bodies must not intersect, otherwise the bodies intersect. The green grids do not intersect the ship projection on the transverse axis of the ship, indicating that the ship is not distributed in two grids. Therefore, the separation axis is constructed along the length and width of the outer tangent rectangular frame of the ship, and the grid within the blue rectangular frame is judged successively whether it intersects with the ship, so as to determine the distribution grid of the ship [19].
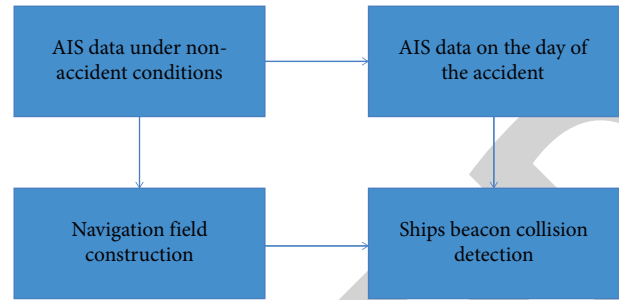

Figure 6: Ship-beacon collision detection flow based on navigation beacon field.
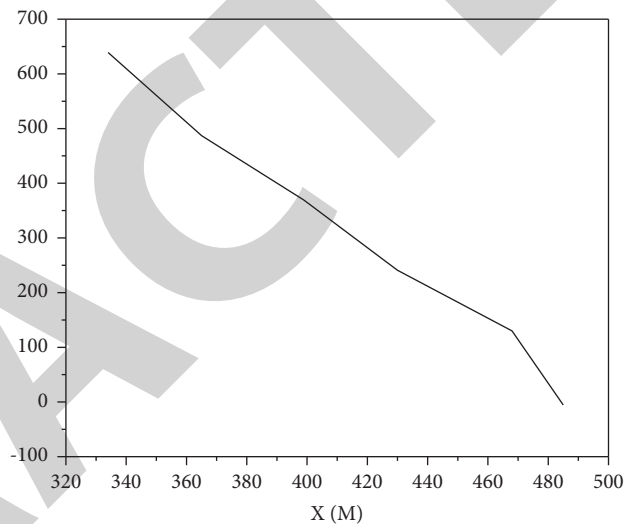

Figure 7: Detection results of the ship involved in the accident of beacon 4431.33.

For the same navigational beacon, the grid distribution results of different ships in the nearby waters were obtained, and the grid distribution results of all ships were superimposed to obtain the statistical results of navigational beacon. Due to the limited data of a single beacon, it is impossible to confirm the range of the beacon field. Multiple grid data of the same size are superimposed to obtain the grid distribution map after being superimposed to ensure the effectiveness of the range of the beacon field. In order to extract the boundary of the navigation mark field, the ship distribution curves in each grid in the four directions of the navigation mark were drawn, respectively, and the critical point of the curve value remaining stable to continuously rising was taken as the distance boundary in each direction. The navigation field is constructed as a circle. The center position of the circle is the position of the navigation beacon, and the radius is confirmed by combining the boundary extraction results and the ship-navigation beacon collision experiment results [20].

4.3. Ship-Beacon Collision Detection Based on Navigation Beacon Field. The navigation mark field constructed above is used to conduct ship-navigation mark collision detection experiment. The experiment includes two contents: collision

detection of all ship tracks matching the track of the ship causing the accident on the day of the navigation mark accident to verify the effectiveness of the range of navigation mark field; Second, collision detection is performed on all ship tracks on the day of the navigation mark accident where the track matching of the ship causing the accident cannot be completed, so as to verify the practicability of the ship-beacon collision detection method based on the navigation mark field. The detection and discrimination of ship-beacon collision can be divided into two types: (1) if the ship point is within the range of $r = 20\,m$ beacon field or there is an intersection between the ship track and $r = 20\,m$ beacon field, the ship can basically be judged as the ship in trouble; (2) If the ship point is within the range of navigation mark $r = 70\,m$ or there is an intersection point between the ship track and navigation mark $R = 70\,m$, there is ship-beacon collision aversion. For the determination of the center position of the navigation mark, based on the AIS data return time point, the prediction point is taken as the center and the navigation mark domain model is used for judgment.

4.3.1. Validation Test of the Model in the Navigational Domain.

Taking navigational beacon 4431.33 as an example, the navigational beacon fields with $R = 20\,m$ and $R = 70\,m$ were tested, respectively, and the results showed that only two ship paths were at the intersection with the navigational beacon fields, as shown in Figure 8. In Figure 8, ship 477269700 is the ship causing the actual ship-buoy collision. The ship first passes through the buoy area and then sails back and forth. Although the ship is close to the buoy, due to its small size (length 40 m, width 12 m), ship-buoy collision does not occur.

Furthermore, the data of the ship's beacon, which cannot be detected in the beacon field of $R = 20\,m$, is tested. Take navigational beacon 4431.22 as an example, there is a ship track that intersects with the field of navigational beacon $r = 20\,m$, as shown in Figure 7. The ship is 150 m long and 22 m wide, and sails in the bow direction without contacting the central navigational beacon. A total of 9 ship tracks were detected in the field of navigational markers with $r = 70\,m$. It is shown that 3 ship tracks were detected with $R = 70\,m$, among which are the tracks of the ship causing the accident. It can be seen that most other nonoffending ship tracks can still be detected in the navigation mark field with $R = 70\,m$.

4.3.2. Practical Test of Ship: Beacon Collision Method.

In order to further verify the practicability of the ship-beacon collision detection method based on the navigation mark field, ship-beacon collision detection is performed on the accident data other than the data matching the ship track and the ship information provided by the navigation mark management department. Taking navigation mark 4560.117 as an example, it is the suspicious ship track detected in the corresponding navigation mark field with $R = 70\,m$, and the two ship tracks are both of ship 412378780. Furthermore, the name of the vessel involved in the accident was queried through the information list of the vessel involved in the accident provided by the navigation beacon management
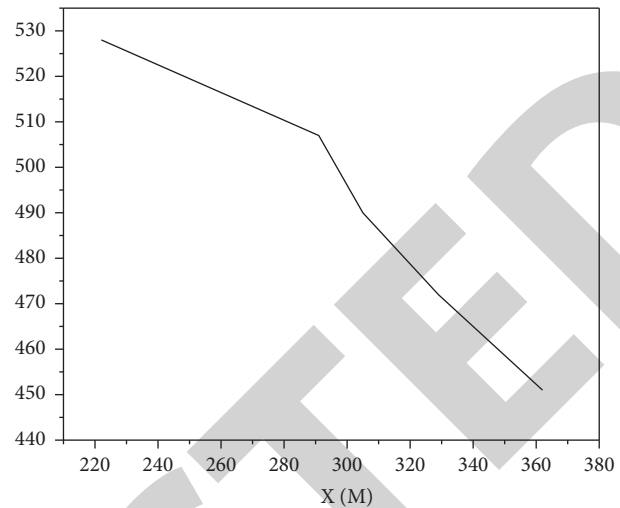

Figure 8: Example of ship detection in accident of navigation beacon 4431.22.

department, and the vessel information network MMSI was used according to the name of the vessel. This verifies the practicability of the ship-beacon collision detection method based on the navigation mark field.

In this article, a ship-buoy collision detection method based on the navigation buoy field is proposed. Through the construction of hierarchical beacon field model, the intersection detection of beacon field and ship track of passing ships is carried out to determine the ship causing the accident. The specific contents include:

(1) The construction process and method of navigational beacon domain based on AIS data are proposed, and the hierarchical navigational beacon domain model is constructed based on ship-buoy collision accident data;

(2) A ship-buoy collision detection method based on hierarchical buoy domain model is proposed, and the effectiveness of the method is verified by actual ship-buoy collision accident data.

However, when multiple ship tracks are detected based on the hierarchical model, it still needs to be judged manually. However, compared with the collision detection method based on trajectory tracking, it avoids the subjective error of relying only on manual judgment, the insufficiency of detecting abnormal data of navigation mark, and the failure of detecting due to the discontinuity of data returned. On the other hand, the collision detection based on fuzzy navigation beacon cannot accurately judge the collision time and location, and does not fully consider the size of the ship.

5. Conclusion

In this article, the lack of systematic and effective detection methods in the actual detection of ship-buoy collision accidents has caused some difficulties in obtaining evidence and tracing responsibility for accidents. Based on the actual ship-beacon collision data and AIS data, ship-beacon

collision methods are studied. The specific research contents and results include the following aspects:

Combining the dynamic characteristics of ship navigation in AIS information with time series, and using longitude, latitude, heading, speed, heading and time increment as inputs, a dynamic prediction model of ship navigation based on LSTM was established. At the same time, PSO-LSTM prediction model based on particle swarm optimization algorithm and GA-LSTM prediction model based on genetic algorithm were constructed to optimize the parameter (step-unit-epoch) optimization in the model, respectively, to help the LSTM network to find the global optimal. The simulation results show that the prediction accuracy of the PROPOSED LSTM model is better than that of the existing BP model. At the same time, the prediction accuracy of the two LSTM models based on heuristic optimization algorithm is better than that of the naive LSTM model, in which the PSO-LSTM model has better performance in the prediction of longitude and latitude, and the GA-LSTM model has better performance in the prediction of ship speed and heading. Therefore, the combination of the two is recorded as LSTM* model to provide a comparative reference for subsequent studies.

Aiming at the deficiency of relying on abnormal data detection and manual judgment in ship-buoy collision detection based on trajectory tracking, a ship-buoy collision detection method based on hierarchical buoy field was proposed based on analyzing the construction process of AIS data–based buoy field. The validity of fuzzy ship domain scope and the practicability of ship-beacon collision detection method are verified by using ship-beacon collision accident data.

Data Availability

The data of this paper can be obtained from the corresponding author upon request.

Conflicts of Interest

The authors declare that they have no conflicts of interest.

Acknowledgments

References

[1] B. Liu, X. Wu, X. Liu, and M. Gong, "Assessment of ecological stress caused by maritime vessels based on a comprehensive model using ais data: case study of the bohai sea, Assessment of ecological stress caused by maritime vessels based on a comprehensive model using AIS data: Case study of the Bohai Sea, Chinahina," *Ecological Indicators*, vol. 126, no. 1, Article ID 107592, 2021.

[2] M. B. Zaman, E. Kobayashi, and A. Zubaydi, "Traffic analysis for enhancing safety in the Traffic analysis for enhancing safety in the Singapore Straits using AIS dataingapore straits using ais data," *IOP Conference Series: Earth and Environmental Science*, vol. 649, no. 1, Article ID 12065, 2021.

[3] Y. Liang and H. Zhang, "Ship track prediction based on ais data and pso optimized lstm network," *International Core Journal of Engineering*, vol. 6, no. 5, pp. 23–33, 2020.

[4] M. Gao and G. Y. Shi, "Ship collision avoidance anthropomorphic decision-making for structured learning based on ais with seq-cgan," *Ocean Engineering*, vol. 217, no. 13–15, Article ID 107922, 2020.

[5] H. T. Lee, J. S. Lee, H. Yang, and I. S. Cho, "An ais data-driven approach to analyze the pattern of ship trajectories in ports using the dbscan algorithm," *Applied Sciences*, vol. 11, no. 2, p. 799, 2021.

[6] J. Xiong, X. Jin, G. Dong, D. Gu, and C. Yi, "Risk assessment of ship traffic safety in port waters based on ais data," *IOP Conference Series: Earth and Environmental Science*, vol. 638, no. 1, Article ID 12022, 2021.

[7] Y. Dogan, O. Kart, B. Kundakci, and S. Nas, "A novel approach for knowledge discovery from ais data: an application for transit marine traffic in the sea of marmara," *Advances in Electrical and Computer Engineering*, vol. 21, no. 3, pp. 73–80, 2021.

[8] W. He, J. Lei, X. Chu, S. Xie, C. Zhong, and Z. Li, "A visual analysis approach to understand and explore quality problems of ais data," *Journal of Marine Science and Engineering*, vol. 9, no. 2, p. 198, 2021.

[9] M. I. Asborno and S. Hernandez, "Assigning a commodity dimension to ais data: disaggregated freight flow on an inland waterway network," *Research in Transportation Business & Management*, vol. 9, Article ID 100683, 2021.

[10] A. A. Masroeri, A. S. Aisjah, and M. M. Jamali, "Iuu fishing and transhipment identification with the miss of ais data using neural networks," *IOP Conference Series: Materials Science and Engineering*, vol. 1052, no. 1, Article ID 12054, 2021.

[11] S. Chen, F. Wang, X. Wei, Z. Tan, and H. Wang, "Analysis of tugboat activities using ais data for the tianjin port," *Transportation Research Record*, vol. 2674, no. 5, pp. 498–509, 2020.

[12] M. Gao and G. Shi, "Modelling of ship collision avoidance behaviours based on ais data," *International Journal of Simulation and Process Modelling*, vol. 15, no. 1/2, p. 100, 2020.

[13] K. Y. Shen, Y. J. Chu, S. J. Chang, and S. M. Chang, "A study of correlation between fishing activity and ais data by deep learning," *TransNav the International Journal on Marine Navigation and Safety of Sea Transportation*, vol. 14, no. 3, pp. 527–531, 2020.

[14] C. Liu, J. Liu, X. Zhou, Z. Zhao, C. Wan, and Z. Liu, "Ais data-driven approach to estimate navigable capacity of busy waterways focusing on ships entering and leaving port," *Ocean Engineering*, vol. 218, no. 2, Article ID 108215, 2020.

[15] G. Dhiman, V. Vinoth Kumar, A. Kaur, and A. Sharma, "Don: deep learning and optimization-based framework for detection of novel coronavirus disease using x-ray images," *Interdisciplinary Sciences: Computational Life Sciences*, vol. 13, no. 2, pp. 260–272, 2021.

[16] J. Jayakumar, B. Nagaraj, S. Chacko, and P. Ajay, "Conceptual implementation of artificial intelligent based E-mobility controller in smart city environment," *Wireless Communications and Mobile Computing*, vol. 2021, Article ID 5325116, 8 pages, 2021.

[17] J. Chen, J. Liu, X. Liu, X. Xu, and F. Zhong, "Decomposition of toluene with a combined plasma photolysis (cpp) reactor: influence of uv irradiation and byproduct analysis," *Plasma*

Chemistry and Plasma Processing, vol. 41, no. 1, pp. 409–420, 2020.

[18] R. Huang, S. Zhang, W. Zhang, and X. Yang, "Progress of zinc oxide-based nanocomposites in the textile industry," *IET Collaborative Intelligent Manufacturing*, vol. 3, no. 3, pp. 281–289, 2021.

[19] Z. Guo and Z. Xiao, "Research on online calibration of lidar and camera for intelligent connected vehicles based on depth-edge matching," *Nonlinear Engineering*, vol. 10, no. 1, pp. 469–476, 2021.

[20] R. Wang, Z. Zhang, Y. Bai et al., "Scanning ion beam etching: a method for the fabrication of computer-generated hologram with nanometric accuracy for aspherical testing," *Optics and Lasers in Engineering*, vol. 139, no. 22, Article ID 106503, 2021.